Csaba FARKAS[1], László FENYVESI[2], Károly PETRÓCZKI[1]

DOI: https://doi.org/10.52091/EVIK-2021/2-5-ENG

Received: August 2020 – Accepted: January 2021

Comparison of the mechanical fatigue indices of Golden Delicious apples and Packham pears

Keywords: fruit damage, TTF (time to failure), rheological testing of fruits, viscoelastic models, time-dependent deformation, loading and unloading curves, dissipated energy, biological yield point, biological rupture point, damage limit value, damage resistance, creep curve, deformation

1. SUMMARY

One of the most significant phenomena in the processing of horticultural crops, leading to the damaging of the fruit, is fatigue due to repeated mechanical stress, which endangers the integrity of the produce, especially during transport. In the event of such damages, the immediate environment of the damaged fruit, or even the entire batch of crops may be in danger, as the biological processes leading to spoilage are not limited to the individual crop damaged. In the case of repeated effects, a force less than the static limit value is sufficient to cause spoilage, but in addition to the load, the material properties of the given crop, as well as the energy balance observed during damage play important roles in determining the mechanical resistance. Accordingly, in our work, a description of the spoilage process is built on the material models most characteristic of the selected crops, on the dissipated energy indicators measured during repeated loads, and on the definition and determination of the spoilage time. In the experiments, the fatigue indices of Golden Delicious apples, making up most of the apple production of the European Union, and of long shelflife Packham pears are compared by setting up linear regression models.

[1] Szent István University, Faculty of Mechanical Engineering, Institute of Process Engineering, Gödöllő
(Since 01. Feruary 2021: Hungarian University of Agriculture and Life Sciences, Institute of Technology)
[2] Szent István University, Faculty of Mechanical Engineering , Institute of Machinery and Informatics, Gödöllő
(Since 01. Feruary 2021: Hungarian University of Agriculture and Life Sciences, Institute of Technology)

Csaba FARKAS	Farkas.Csaba@uni-mate.hu	https://orcid.org/0000-0002-0832-9973
László FENYVESI	Fenyvesi.Laszlo@uni-mate.hu	https://orcid.org/0000-0002-0832-9973
Károly PETRÓCZKI	Petroczki.Karoly@uni-mate.hu	https://orcid.org/0000-0003-3331-8499

2. Introduction

When sorting produce, not only the size and shape, but also the extent of a possible damage or, in many cases, the fact of the damage itself is the basis for the selection. Automated machine recognition, which in most cases is performed by spectral imaging methods, today can effectively separate damaged crop tissues from healthy ones and finding damages under the surface which are not visible to the naked eye does not pose a problem to the technology either **[1, 2]**. Reliability depends on the hardware design (i.e., the accuracy of the equipment used) on the one hand, and on the algorithms used **[3]**. In addition to sorting, the method also uses camera monitoring, which can take into account the ripeness of tomatoes with the help of the appropriate software, and which allows the fully automated operation of the harvesting robots **[4]**.

Although with effective detection the damaged crops can be easily removed from the processing chain, in addition to screening, the objective of getting as many healthy goods as possible to customers after the harvest, and the necessary treatment processes must also be kept in mind. Since international surveys show that a significant proportion of crops does not reach consumers in the market due to losses at different stages of processing **[5, 6, 7]**, in addition to the precise detection of injuries, prevention must also play a key role. This also requires destructive testing of the crops and the direct observation of spoilage processes.

The material properties of various agricultural and horticultural crops can be described using viscoelastic models, consisting partly of elastic and partly of viscous components. Complex material structures can also be built from basic elements connected in a serial or parallel way, and of the three-element systems, the Poynting-Thomson model has been used several times in previous research to characterize Maloideae **[8, 9, 10]**. In the case of viscoelastic systems, deformation due to mechanical interactions depends not only on the magnitude of the stress, but also on the speed of the load, and creep and relaxation are an important part of the load and deformation process: while in the case of the former, a constant load results in increasing deformation, in the case of the latter phenomenon, a constant deformation results in a continuous decrease in stress **[11]**.

The reaction of a given crop to a mechanical impact is shown on the load-deformation curve which, in addition to the creep and relaxation parameters, provides information on the total amount of energy generated in the load process: the area enclosed by the load and unload curves also serves as the basis for dissipated energy calculations in other fields **[12, 13]**, and it is closely related to the viscoelastic properties of the test material and, in the case of crops, to the mechanical resistance and the susceptibility to damages **[14]**.

The load limit that leads to microscopic damage to the cell structure, which can also cause crop spoilage, is called the biological yield point. Although as biological materials, different crops may be capable of healing or even complete regeneration, mechanical impacts applied during processing should be kept below the biological yield point. The limit value can also be indicated by a damage visible to the naked eye and affecting a larger area, which is called the rupture point in the literature. In the case of such damages, the crop is very likely to spoil **[15, 16]**. There is usually a significant variance between damage limits (even in the case of the same exact load), which is also affected by the ripeness of the given crop, as well as the conditions provided during storage and processing.

In additions to collisions resulting from improper handling, most damages are caused by vibrations during transport. Unfortunately, the observation of processes that end in damages by destructive tests is not an area that today's research focuses on, although the mapping of fatigue due to repeated loads is also essential in fruits **[17]**.

During transport simulations, the frequencies causing the greatest damage have already been unanimously identified **[18, 19, 20]**, so in the case of destructive tests with repeated loads, experience shows that it is advisable to set the frequency range below 10 Hz.

Multivariate regression models that take into account different test parameters are often used to describe the mechanical properties of fruits and vegetables **[21, 22]**. The objective of our research was to study the less discussed phenomenon of fatigue in crops, and to determine the relationship between damage limit values (biological yield point or rupture point) and related factors (energy balance, material properties). The goal was to establish a linear equation for the damage limit value, which is determined by considering the parameters that can be measured during repetitive compressive load.

3. Materials and methods

3.1. Measuring instrument and the securing of the fruits

Destructive tests were performed with the instrument called DyMaTest, provided by the Hungarian Institute of Agricultural Engineering of NAIK. The instrument applies a load to the fruit with a cylindrical (flat-faced) pressure pin, and the pressure force can be adjusted arbitrarily using the software interface developed for the instrument **[23]**. The deformation of the crop can be registered with a laser sensor that detects the movement of the measuring pin, and the force can be registered with a special measuring cell designed for the instrument. Tests were performed after setting a sinusoidal pressure force up to the fruit failure limit.

To perform the measurements, the crops were secured in a sand bed. To check that the creep of the sand applied did not affect the results obtained, control measurements were performed using a completely inelastic bearing ball with a diameter of 32 mm. During the compressive loads, there was no detectable displacement in the measuring range of the photoelectric sensor, so the deformation of the sand does not appear on the load curves of the fruits at all. Prior to testing, sand preparation consisted of wetting, sieving and compaction operations **[24]**.

3.2. Crop deformation curves

For the tests with repetitive loads, a cyclic waveform was used, which can be characterized by the following function:

$$F_m = F_{max}\,(1 - \cos(\omega t)),$$

where F_{max} is the peak value of the periodic load function [N] and ω is the angular velocity of the load [s^{-1}].

The resulting deformation due to periodic loading is also periodic. ***Figure 1.a*** shows the time function of the deformation of a Golden apple, while ***Figure 3.b*** shows the force-deformation curve. Typical deformation curves for Packham pears are shown in ***Figures 3.c*** and ***3.d***.

As a result of the cyclic load with a constant amplitude, the deformation changes continuously, and this can be noticed in the increase of the envelope (or the mean). Since these envelopes increase similarly to the creep curves observed under static loading, this process is called dynamic creep **[25]**.

The response function to the cyclic load can be described by the following equation:

$$w_m = \beta + w_{max}\,(1 - \cos(\omega t - \delta)),$$

where w is the deformation [mm], β is the creep term, w_{max} is the peak value of the periodic deformation function [mm], ω is the angular velocity [s^{-1}], and δ is the phase shift between the load and deformation time functions.

To characterize creep (in this case, to give), the literature generally uses a linear approximation. Although this approximation may be appropriate for a significant region of the creep in most cases, the initial and failure sections of the curve cannot be linearized, so the method carries inaccuracies when considering the entire creep process. In order to avoid this, numerical solutions were used in the data management processes related to deformation, in which the operations were performed not by approximation, but by direct processing of the data series.

In the case of the curves shown in ***Figure 1***, the damage limit of the fruits, in this case the rupture point, has already been determined, and the data after this point have been removed from the diagrams. By analyzing the curves obtained this way, we can actually obtain information about the energy conditions taking place until failure, as well as about the material properties experienced this far.

Since the rupture point cannot be distinguished clearly during the analysis of the diagrams in many cases, especially in the case of loads that take place rapidly and the concomitant sharply changing deformation processes, accurate determination was therefore performed by high frame rate video surveillance ***(Figure 2)***. The camera used recorded 240 frames per second, and the rupture point sought was the first frame of the failure phase, when the pressure pin visibly exits the slowly increasing deformation range during the creep phase and causes damage to the crop tissue that is visible from the outside by breaking the skin. In this case, both the skin and the flesh are damaged, so the material behavior is approximated by the modeling of not a structure with a homogeneous composition, but of a „structure".

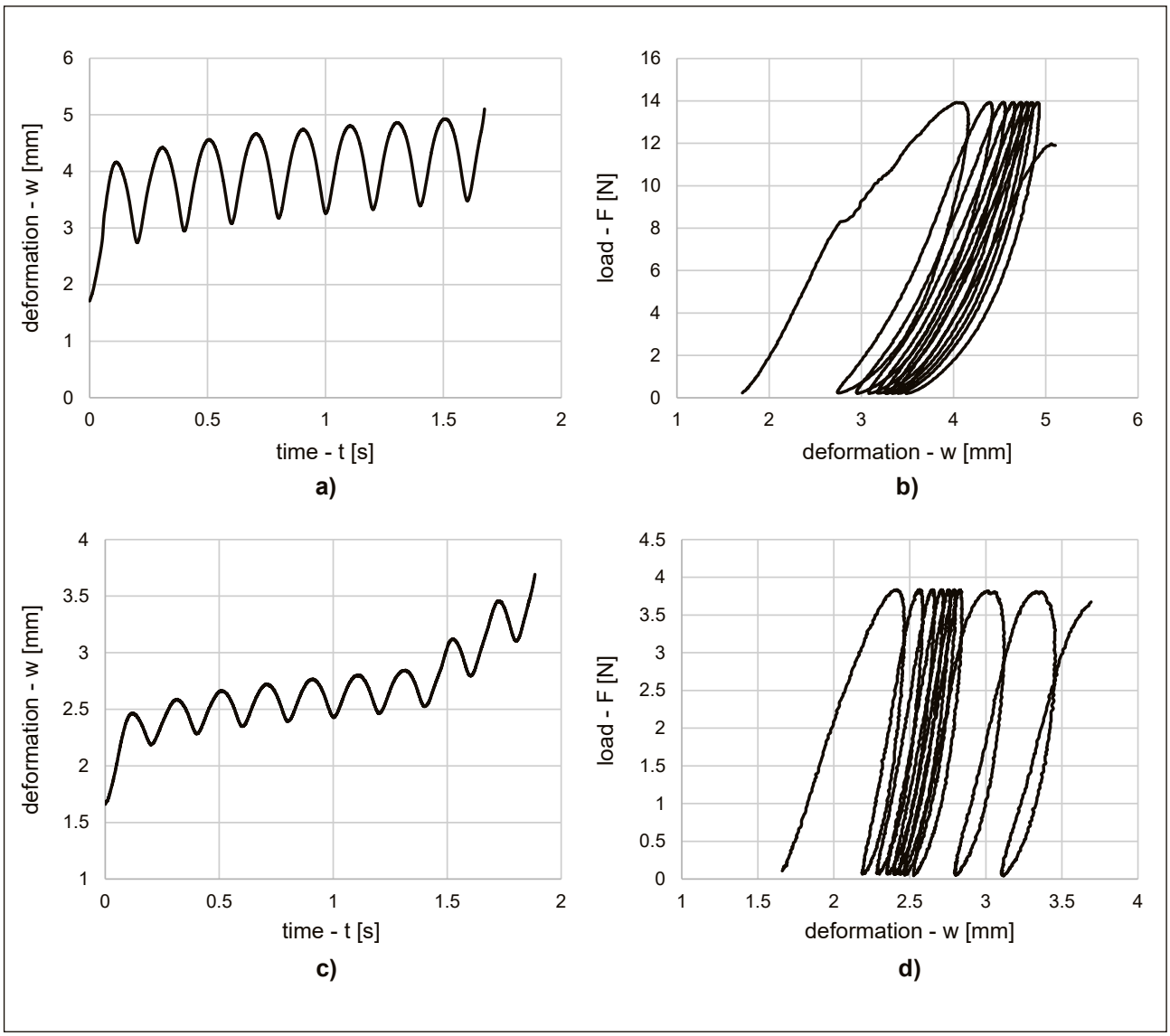

Figure 1. Time vs. deformation (a) and force vs. deformation (b) functions of a Golden Delicious apple, and time vs. deformation (c) and force vs. deformation (d) functions of a Packham pear
Deformation – Time – Force

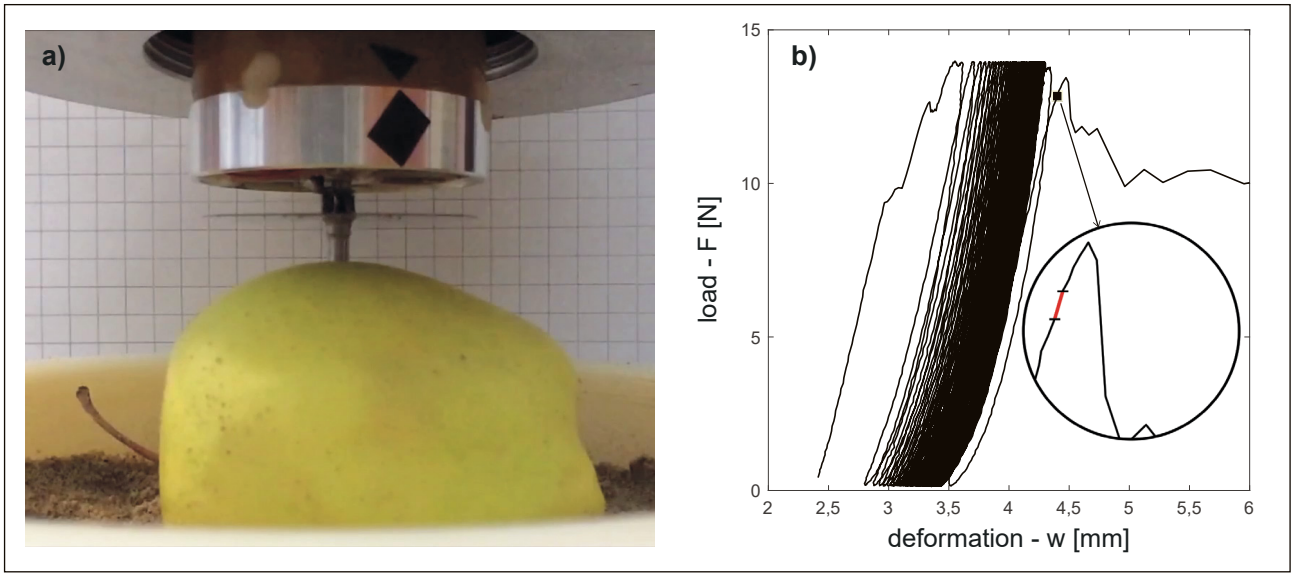

Figure 2. Determination of the rupture point by analyzing high frame rate recording
Force - Deformation

The sampling frequency of the DyMaTest is 2 kHz, which is 8.3 times higher than that of the video recordings of the rupture point. The absolute error of the frame analysis compared to the data collected by the material testing instrument is 4.16 milliseconds, which is the lowest resolution unit of the camera. ***Figure 2.b*** illustrates the error range for the rupture point. The rupture point as a test parameter is hereinafter denoted by the notation , which refers to the term *time to failure*.

3.3. Viscoelastic material properties

To determine the material properties of fruits, the three-element Poynting-Thomson model was used, which had already been used in previous research projects on apples. The coupling of the model is shown in ***Figure 3***, and it can be characterized by the following equation:

$$F_m + \frac{\eta}{E_1+E_2}\dot{F_m} = \frac{E_1E_2}{E_1+E_2}w_m + \frac{E_1\eta}{E_1+E_2}\dot{w_m},$$

where E_1 and E_2 are the elastic components of the mechanical model [N mm^{-1}] and η is the viscous element [Ns mm^{-1}]. F_m is the compressive force recorded during the measurements [N] and w_m is the deformation obtained during the measurements [mm].

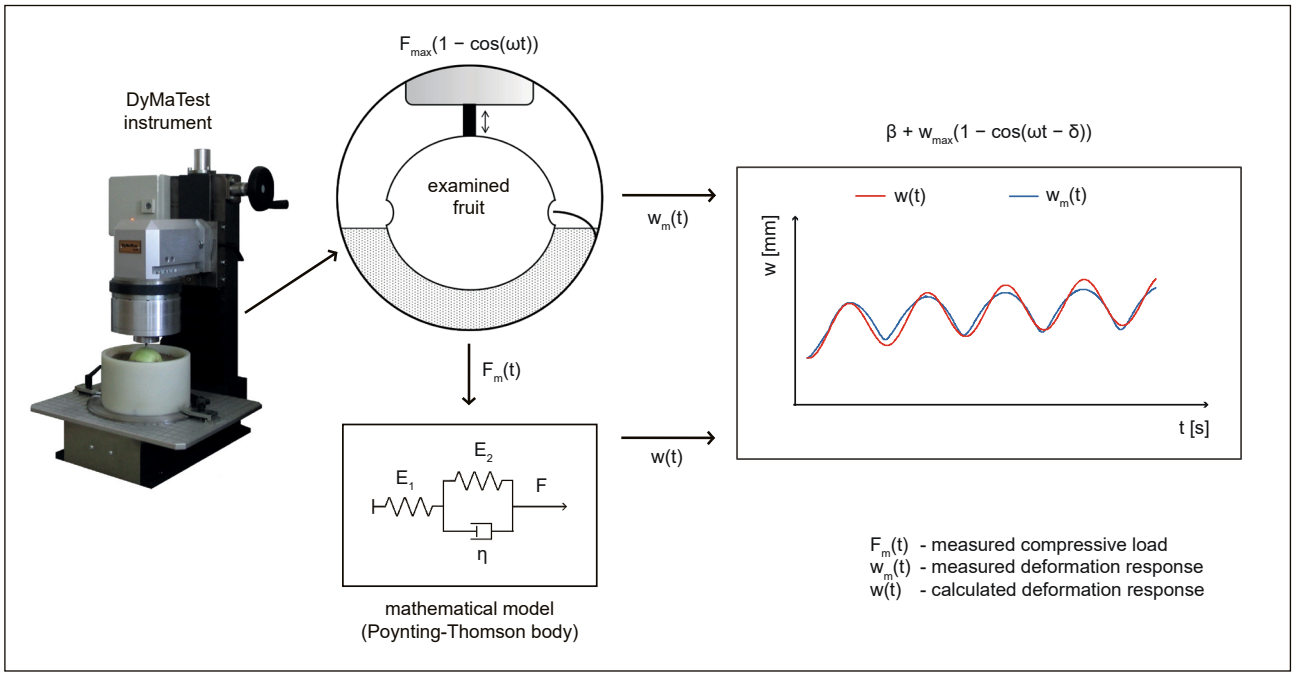

Figure 3. Identification of the computer mathematical model
DyMaTest material testing equipment - Investigated crop - Mathematical model – Measured compressive load – Measured deformation – Calculated deformation

The block-oriented writing of the equation was performed in a Matlab Simulink environment, where the model was identified with the force and deformation data obtained during the measurements ***(Figure 3)***. The values of the elastic and viscous coefficients were determined for the calculated curve (w) that best fit the measured results (w_m). To minimize the difference between the two data sets, we used a procedure based on the least square method:

$$\int_0^T (w_M(t) - w(t))^2\, dt \longrightarrow min.$$

After running the minimum search process, the model coefficients E_1, E_2 and η were recorded and were used as test parameters. The approximations carried out with the presented mathematical system provided R^2 values between 0.967 and 0.998.

3.4. Analysis of the hysteresis curves

The force vs. deformation diagrams in ***Figures 1.b, 1.d*** and ***4*** show recurrent hysteresis processes where the area enclosed by the load and unload curves is closely related to the energy indices of the crop for the given cycle. The horizontal axis shows that the curve does not close after unloading, so a w_M permanent deformation occurs in the material in each cycle until the next compressive load, and the w_R elastic deformation of the given crop is due to the difference between the load peak and the permanent deformation (the sum of the two gives the total magnitude of the deformation in the given cycle).

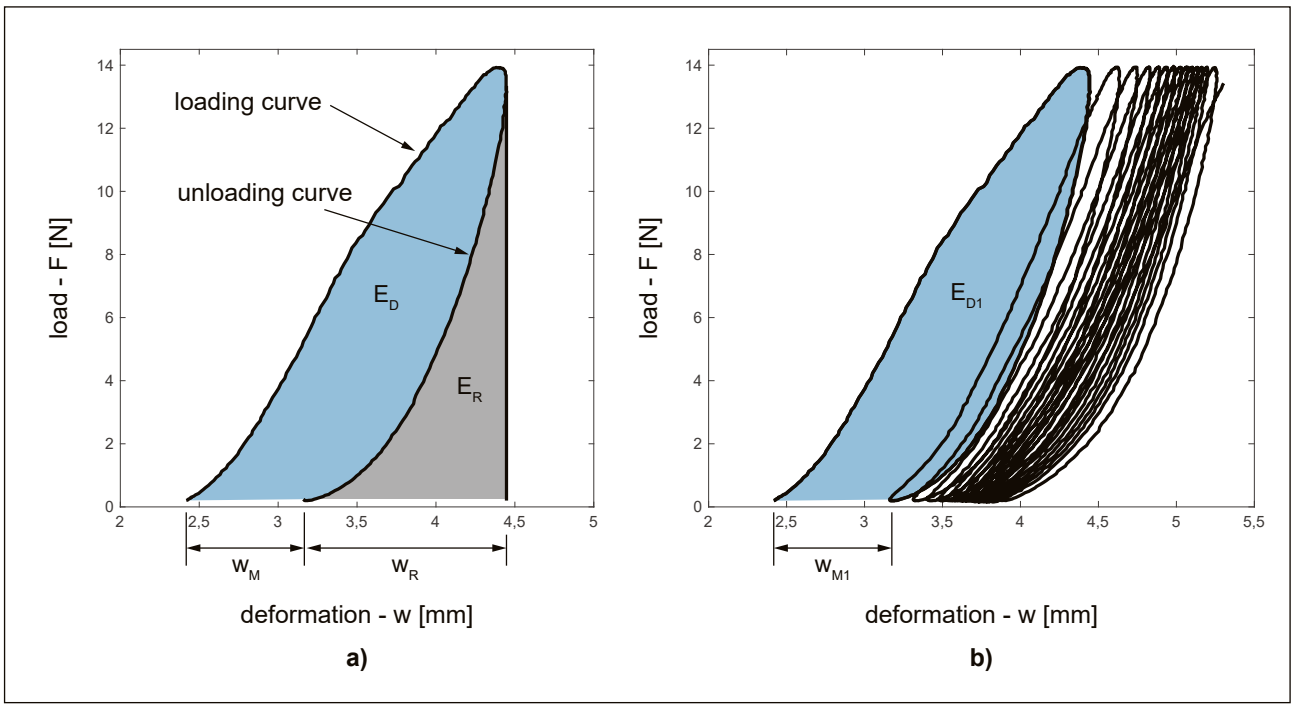

Figure 4. Force vs. deformation curve of a single load cycle (a) and the force vs. deformation curve until failure of a crop (b) for a Golden Delicious apple
Load – Unloading - Deformation

If we examine the areas between the curves, by subtracting the energy associated with the elastic deformation () from the total work (), the dissipated energy of the cycle () is obtained. This energy loss can be calculated by determining the area between the curves:

$$E_D = \int_0^{t_{wM}} F \frac{dw}{dt} dt ,$$

where t_{w_M} is the time elapsed between the start of the loading process and the end of the unloading [s] and F is the load function produced by the test equipment [N].

Since the area calculation was performed by the numerical integration of the force and deformation data over time, the previously mentioned approximation functions and their inaccuracies associated with them can be avoided.

Although the calculation of energy losses is included in several studies that describe the damage mechanism, only a portion of the dissipated energy that can be determined from the hysteresis curve is related to material damage and the failure process **[13]**. In other fields, such as the rheological description of pavement asphalt layers, calculation methods have also been developed that point directly to the moment of failure using the dissipated energy data. These include the so-called dissipated energy quotient, which can be calculated by the following equation **[26]**:

$$E_{DR} = \frac{\sum_{i=0}^{n} E_{Di}}{E_{Dn}},$$

where E_{Di} is the total energy loss up to the given cycle [N mm] and E_{Dn} is the energy loss of the given cycle [N mm].

When the dissipated energy quotient is plotted as a function of the number of cycles ***(Figure 5)***, it can hint at two damage indicators: the onset of the cracking process of the given asphalt is indicated by a 10% drop in the ramp-up slope of the curve, and the fracture seen at the peak is the fatigue failure **[26]**.

In the course of our experiments on fruits, the said drop in the slope cannot be observed so clearly in most cases, which is probably a consequence of the rapid load settings. However, the internal rupture point clearly appears in our own results as well. In addition to the time elapsed until the rupture point and the viscoelastic model coefficients, this data is also used to construct the equations describing the damage process.

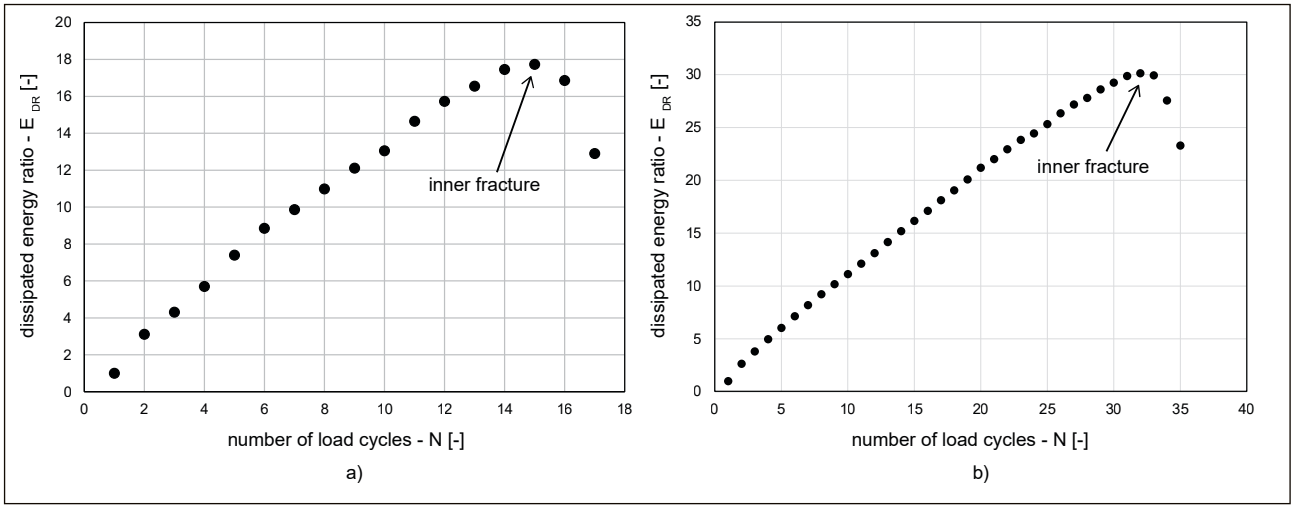

Figure 5. Internal rupture point indicating fatigue based on the quotient calculated from dissipated energies for a Golden Delicious (a) and a Packham (b) produce
Ratio of dissipated energy – Internal breaking point – Number of load cycles

3.5. Test parameters, load settings

Our objective was to describe, using parameters related to the damage process, the time to failure (), which will be a dependent variable of the resulting equations. When characterizing failure, we aim to establish linear regression equations.

Compressive loads were applied to 25 Golden Delicious apples and 25 Packham pears (i.e., the number of replicates for each crop was 25), and six different measurement frequencies were used for each fruit. These frequencies fall into the range considered to be the most dangerous in transportation research, mainly in the range below 10 Hz, and taking into account the setting options of our instrument, they were 2.5, 3.7, 5, 7.5, 10 and 11.6 Hz. Thus, a total of 300 compressive loads were applied, and from the force, deformation and time data obtained during the loads, the E_1, E_1 and η coefficients of the material model were determined in each case, as well as the *TTF* time to failure and the E_{DRmax} internal damage index, using the methods detailed above. In addition, it is also taken into account whether the process was influenced by the test frequencies.

Because of the different load resistance of the Golden and Packham crops, different compressive forces had to be applied: in the case of Packham pears, failure was already reached in one of the first cycles at certain values of the frequency range, while Golden apples were much more resistant, so considering the compatibility of the damage times and dissipated energy values to be detailed later, a load of 4 N to pears and a load of 14 N was applied to apples. In practice this means that at settings greater than 4 N, for most of the frequency values investigated, immediate destruction occurred in pears, and in the case of settings below 14 N, load processes orders of magnitude longer would have to be run to visibly damage the apples.

4. Results

4.1. Times to failure and energy indicators hinting at internal damage

Average and standard deviation values of the ties to failure for each frequency setting are shown in ***Table 1***. ***Figure 6.a*** shows a chart of the average values of Golden apples, while for Packham pears, the results are shown in ***Figure 6.b***. In the case of apples, the rupture points occurred as expected, i.e., irreversible damage occurred earlier at higher frequencies, while there was a deviation from this in the average values obtained for pears, as at settings above 5 Hz, there is an increasing trend can be seen in time to failure.

Table 1. Average times to failure and standard deviations of the results

Frequency [Hz]	Golden		Packham	
	TTF [s]	Standard deviation – s_{TTF} [s]	TTF [s]	Standard deviation – s_{TTF} [s]
2.5	6.002	3.006	1.522	1.105
3.7	3.758	1.857	1.237	0.858
5	2.505	1.383	1.203	0.847
7.5	1.639	0.762	1.451	1.114
10	1.192	0.672	2.046	1.662
11.6	0.938	0.938	3.384	2.790

In the case of the Golden apples, larger standard deviation values can be found at lower frequency settings, while at higher frequencies, the extreme values of the error ranges move closer to the average values. The endpoints of the standard deviation range show a similar trend to the frequency dependence of the average in Golden apples, but in the case of pears, the minimum values of the standard deviation range no longer represent the change in the average values, thus different characteristics are observed for pears between the 25 measurements.

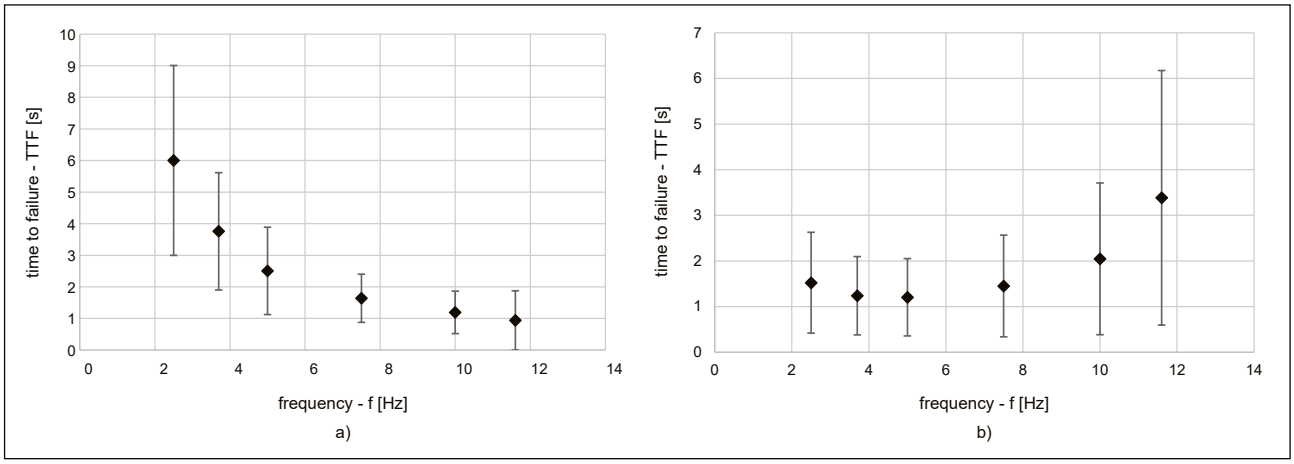

Figure 6. Frequency dependence of the times to failure for Golden Delicious apples (a) and for Packham pears (b)
Failure time - Frequency

Since the standard deviation is quite significant for both apples and pears ***(Table 1)***, the role of the additional parameters considered in the study (viscoelastic model coefficients, as well as energy indices) is particularly important when considering their effect on the damage process during the description of time to failure.

Figure 7 shows the peak values of the energy loss quotient calculated from the dissipated energy, and the results for 25 crops each were also averaged for each frequency setting.

In the case of the Golden apples examined, both the energy loss values recorded for each cycle and the maximum quotient values indicating internal rupture show a decreasing trend towards higher frequency settings, however, in the case of pears, this process is reversed, and the trend describing the frequency dependence also has a different nature.

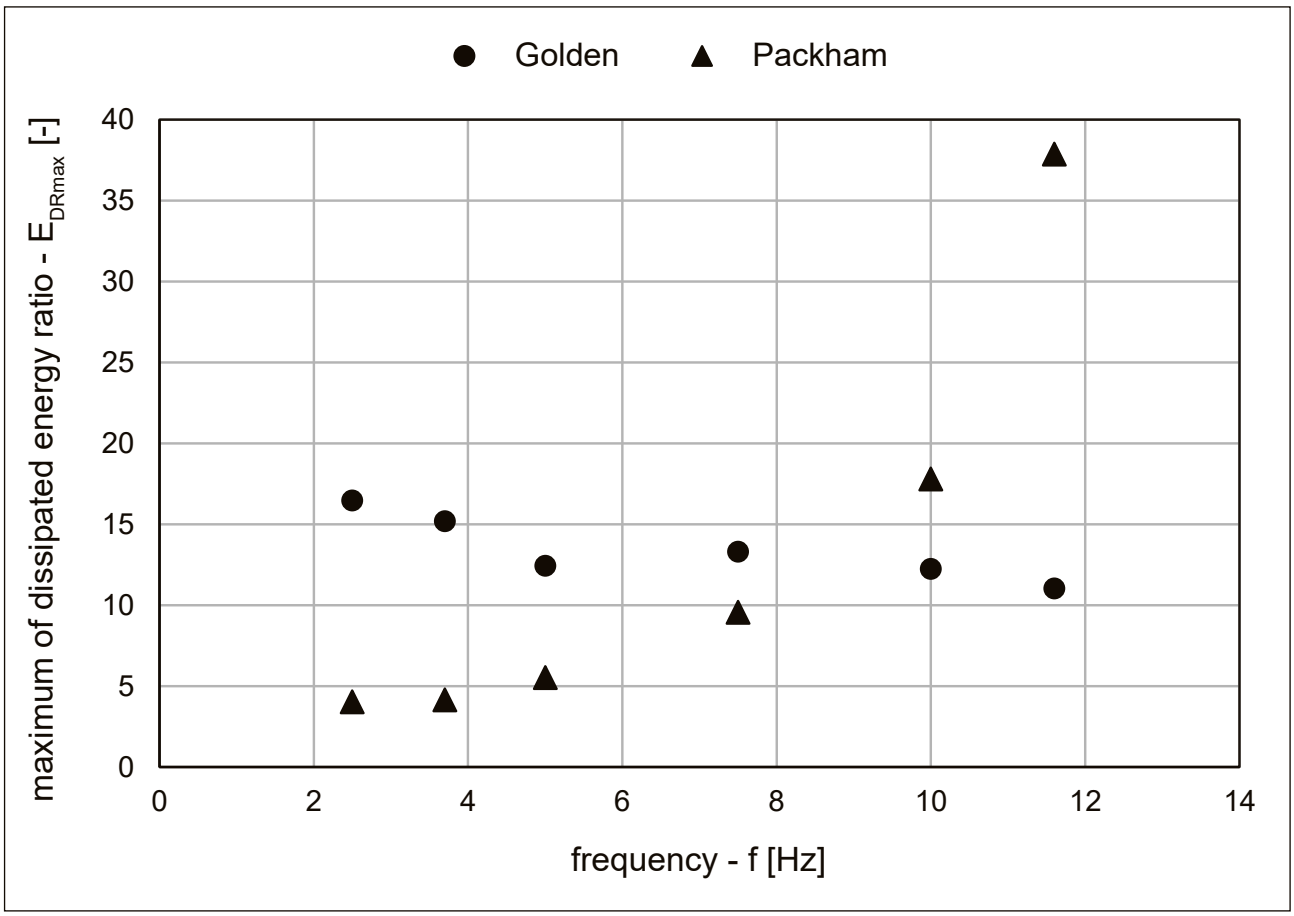

Figure 7. Frequency dependence of the average values of accumulated dissipated energy Maximum of dissipated energy ratio

4.2. Evaluation of viscoelastic model parameters

The frequency dependence of the elastic (,) and viscous () material properties of the crops is shown in ***Figure 8***, where the values of each series of measurements are displayed averaged at each frequency setting. Numerical results are summarized in ***Tables 2 and 3.***

Table 2. Average values and standard deviations of viscoelastic model parameters at each load frequency for Golden Delicious apples

Golden						
f [Hz]	**E_1 [N mm^{-1}]**	**E_1 standard deviation [N mm^{-1}]**	**E_2 [N mm^{-1}]**	**E_2 standard deviation [N mm^{-1}]**	**η [Ns mm^{-1}]**	η standard deviation **[Ns mm^{-1}]**
2.5	10.504	1.250	2.139	0.277	2.129	0.703
3.7	10.523	1.091	2.158	0.277	1.429	0.358
5	10.546	1.497	2.116	0.292	1.109	0.251
7.5	10.622	1.529	2.139	0.269	0.722	0.204
10	10.271	1.177	2.167	0.206	0.581	0.154
11.6	9.848	1.310	1.984	0.361	0.509	0.106

Table 3. Average values and standard deviations of viscoelastic model parameters at each load frequency for Packham pears

Packham						
f [Hz]	**E_1 [N mm^{-1}]**	**E_1 standard deviation [N mm^{-1}]**	**E_2 [N mm^{-1}]**	**E_2 standard deviation [N mm^{-1}]**	**η [Ns mm^{-1}]**	**η standard deviation [Ns mm^{-1}]**
2.5	6.896	1.710	0.554	0.160	0.848	0.494
3.7	7.705	2.184	0.518	0.177	0.574	0.226
5	7.695	2.243	0.565	0.135	0.479	0.242
7.5	8.981	1.873	0.600	0.192	0.435	0.223
10	9.730	2.540	0.613	0.130	0.436	0.243
11.6	10.178	2.172	0.623	0.127	0.471	0.239

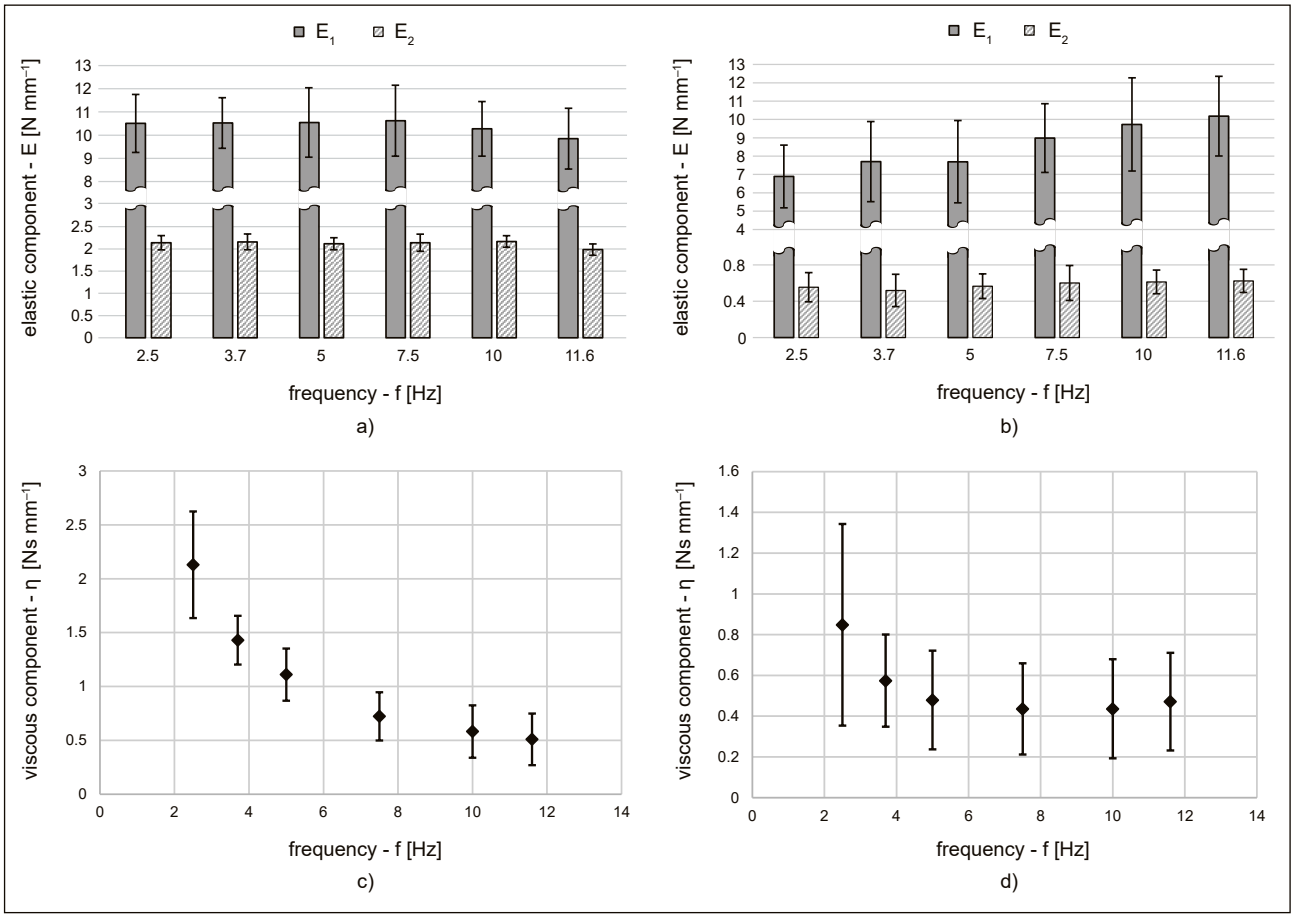

Figure 8. Averages of elastic and viscous model parameters for Golden apples (a, c) and Packham pears (b, d) Viscous element - Frequency

The elastic coefficients in the case of Golden apples do not exhibit an apparent frequency dependence, while a slight decrease can be detected in the case of the E_1 parameters when higher test frequencies are used. In previous experiments, apples tended to behave more rigidly at higher load velocities **[25]**: if a higher load velocity corresponds to a higher frequency in the present case, then this reaction is consistent with the earlier experience.

However, in the case of pears, there is a clear increase when component E_1 is examined, and this result may explain the obtained time to failure data: at the frequencies above 5 Hz, a more elastic, softer surface is formed near the load zone in the pears examined, and the increased elasticity provides a more favorable mechanical resistance for the crops. Thus, in the most dangerous frequency range, higher values do not necessarily carry the most significant damage potential. The E_2 elastic coefficient is constant in the studied range for both Golden apples and Packham pears.

By plotting the viscous parameters, a clear frequency dependence is obtained for both Golden apples and Packham pears. The curve obtained for apples shows a similarity to the frequency dependence of a dynamic viscosity factor presented in a previous research **[27]**, while in the case of pears, also the frequency around 5 Hz breaks the downward trend, this may also be related to the rupture point in the frequency curve of the times to failure.

The error ranges showing the standard deviations are wider in the case of pears, the widest range of standard deviation was recorded at the 2.5 Hz setting. One of the reasons for this is that with this setting, several pears were already destroyed in the first loading phase of the first cycle.

Table 4. Analysis of variance of viscoelastic model parameters

Golden			Packham		
Coefficient	**F**	**p**	**Coefficient**	**F**	**p**
E_1	1.196	0.314	E_1	8.008	<0.001
E_2	1.408	0.225	E_2	1.488	0.198
η	75.393	<0.001	η	6.427	<0.001

The degree of frequency dependence was checked by analysis of variance (ANOVA) and the results are summarized in ***Table 4***. In the case of Golden apples, a significant correlation can only be detected for coefficient η ($p<0.05$), and this confirms the conclusion that can be drawn from the diagrams, which were reached in the case of coefficients E_1 and E_2: the elastic elements and the frequency in the studied range are not detectably related. In the case of Packham pears, however, in addition to η, the frequency dependence of the elastic coefficient E_1 can also be detected, which plays a significant role in the mechanical resistance experienced above 5 Hz.

4.3. Linear failure models

Using the results of the tests presented and the values of the load frequencies, the possibility of four different failure modes for Golden Delicious apples is suggested, according to the following search function:

$$TTF = A + B\eta + CE_{DRmax} + Df + KE_1 + JE_2,$$

where *A*, *B*, *C*, *D*, *K* are *E* constants. The different versions are described in ***Table 5***. These include the elastic and viscous material properties of the crops, as well as the peak value of the dissipated energy, but not the frequency settings.

Table 5. Linear models that can be created from the measured parameters for Golden apples

Model	R	R^2	Modified R^2	Standard deviation of the estimate	Change in R^2	Change in F	Change in the significance of F
1	0.902(a)	0.814	0.812	1.03413	0.814	641.502	0.000
2	0.963(b)	0.927	0.926	0.64922	0.113	226.984	0.000
3	0.971(c)	0.943	0.941	0.57824	0.015	39.039	0.000
4	0.972(d)	0.945	0.943	0.56840	0.002	6.064	0.015

(a) variable: η
(b) variables: η, E_{DRmax}
(c) variables: η, E_{DRmax}, E_1
(d) variables: η, E_{DRmax}, E_1, E_2

In the curves showing the model parameters and as the result of the analysis of variance, there was no significant relationship between the elastic coefficients and the frequency, but the elasticity for the Golden apples had a clear effect on the failure process, resulting in a detectable increase. While the elastic coefficient E_1 is a defining part of the equation, E_2 contributes only negibly to the accuracy of the fit, so we chose the third equation for the simplest description of the failure of Golden apples:

$$TTF = 0{,}533 + 2{,}736\eta + 0{,}141E_{DRmax} - 0{,}261E_1.$$

The models applicable to Packham pears are summarized in ***Table 6***. In these versions, the load frequency appears as well, playing an important role in the description of the time to failure.

Table 6. Linear models that can be created from the measured parameters for Packham pears

Model	R	R^2	Modified R^2	Standard deviation of the estimate	Change in R^2	Change in F	Change in the significance of F
1	0.886(a)	0.785	0.783	0.66044	0.785	488.514	0.000
2	0.933(b)	0.871	0.869	0.51404	0.086	88.193	0.000
3	0.946(c)	0.896	0.893	0.46299	0.025	31.948	0.000
4	0.959(d)	0.920	0.917	0.40765	0.024	39.273	0.000

(a) variable: E_{DRmax}
(b) variables: E_{DRmax}, η
(c) variables: E_{DRmax}, η, f
(d) variables: E_{DRmax}, η, f, E_2

Although the parameter E_1 was related to the frequency, failure is not affected by this coefficient, but E_2 connected in parallel with the viscous component. Since both the frequency and the elastic factor E_2 contribute significantly to the accuracy of the linear approximation, a fourth equation was written for Packham pears:

$$TTF = 0{,}091 + 0{,}788\eta + 0{,}085E_{DRmax} - 0{,}103f + 1{,}524E_2 .$$

The results of the analysis of variance checking the validity of the equations are shown in ***Table 7***. Since the F values obtained are considered to be significant ($p<0.05$), the approximations described are valid.

Table 7. Analysis of variance of the approximation equations

Golden		Packham	
F	p	F	p
792.307	<0.001	375.742	<0.001

Time to failure results (TTF_{sz}) of the models generated after substitution, as well as their relationships to the measured results (TTF_m) are shown in ***Figure 9*** over the entire study range. Averaged results by frequency of the approximation applied to Golden Delicious apples were between 1.54% and 3.85% relative error, while the results averaged by crop were between 1.01% and 31.13%. For Packham pears, averaging the results obtained for each frequency setting, the relative errors were between 2.42% and 6.22%, while the deviations of the values calculated for individual crops were between 0.04% and 34.51% compared to the measured time to failure. The higher error values were not related to the given frequency settings, but to the different mechanical resistance and material properties of each crop.

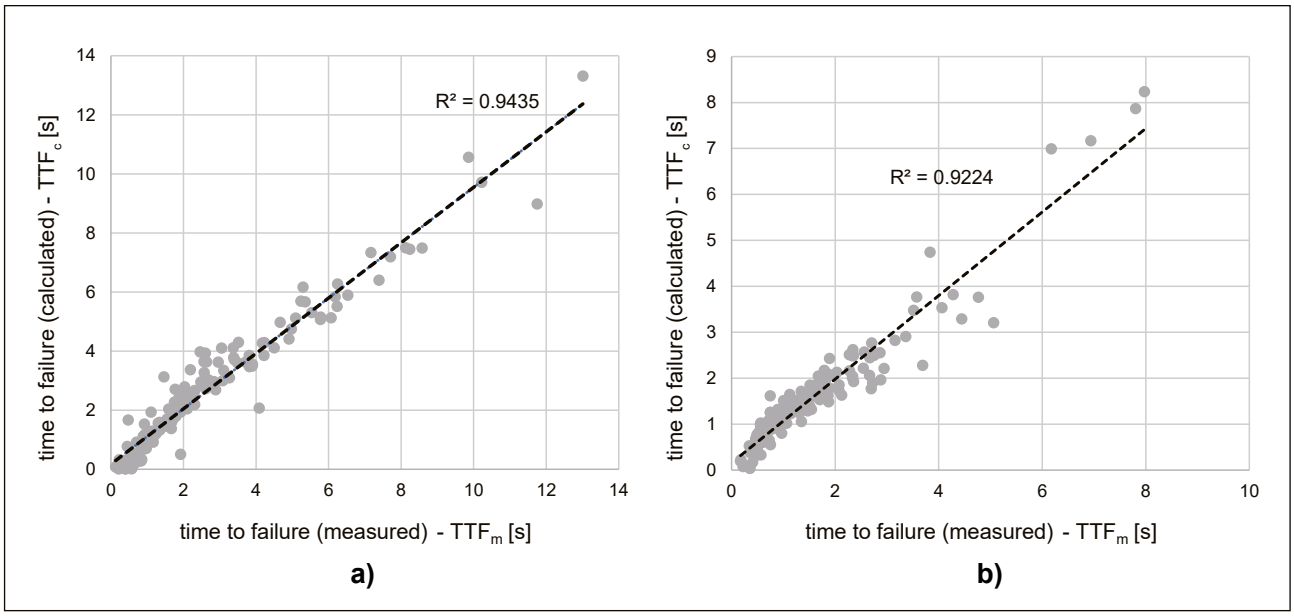

Figure 9. Relationship between measured and calculated times to failure for Golden Delicious apples (a) and Packham pears (b), evaluating all measurement results
Faliure time (measured) - Faliure time (calculated)

5. Conclusions

Repetitive loading during fruit processing and transport procedures causes significant damage, so in our work we investigated failure caused by fatigue, and to this end we developed multivariate linear regression models based on the most important material properties and energy indices related to the failure process, and which can predict the damage resistance of the tested Maloideae (Golden Delicious apples and Packham pears).

In some cases, the rupture point indicating failure cannot be evaluated from the deformation data obtained during the measurements, in which case limit values determined by rapid filming and frame analysis may be helpful during the analyses. The accuracy of this depends on the frame refresh rate of the cameras used, and this, together with image resolution, is constantly evolving in mobile devices, so these devices are also becoming suitable for similar measurement tasks, and their use in the monitoring of the deformation of fruits is no longer unprecedented.

Observing internal damage on the basis of energy calculations may represent a new research direction in the study of fruit damages, as environmental impacts in processing procedures need to be addressed accordingly (limitation or modification of handling, dropping and vibration limit values). However, a precise definition of the phenomenon in order to describe the damage process in the cellular structure in more detail is still awaiting microlevel investigation and confirmation.

6. Acknowledgment

The authors would like to thank the Institute of Agricultural Mechanization of NAIK for providing the DyMaTest material testing instrument. We would also like to thank Dr. László Földi for his help in computer modeling and Dr. László Székely for his help in establishing the multivariate equations.

7. References

[1] Che, W., Sun, L., Zhang, Q., Tan, W., Ye, D., Zhang, D., Liu, Y. (2018): Pixel based bruise region extraction of apple using Vis-NIR hyperspectral imaging. Computers and Electronics in Agriculture 146, pp. 12-21. https://doi.org/10.1016/j.compag.2018.01.013

[2] Tan, W., Sun, L., Yang, F., Che, W., Ye, D., Zhang, D., Zou, B. (2018): Study on bruising degree classification of apples using hyperspectral imaging and GS-SVM. Optik 154, pp. 581-592. https://doi.org/10.1016/j.ijleo.2017.10.090

[3] Gergely, Z., Beke, J. (2015): Az osztályozási hibák csökkentésének lehetőségei a HPV-I sorozatú paprikaválogató gépeken, Mezőgazdasági Technika 2015/11, pp. 2-4.

[4] Malik, M., Zhang, T., Li, H., Zhang, M., Shabbir, S., Saeed, A. (2018): Mature Tomato Fruit Detection Algorithm Based on improved HSV and Watershed Algorithm. IFAC-PapersOnLine 51 (17) pp. 431-436. https://doi.org/10.1016/j.ifacol.2018.08.183

[5] FAO, (2011): Global Food Losses and Waste. Extent, Causes and Prevention. http://www.fao.org/docrep/014/mb060e/mb060e00.pdf (Hozzáférés / Aquired: 12.08.2020)

[6] NRDC, (2012): Wasted: How America is losing up to 40 percent of its food from farm to fork. NRDC Issue PAPER. https://www.nrdc.org/sites/default/files/wasted-food-IP.pdf (Hozzáférés / Aquired: 12.08.2020)

[7] Yahia, E. M., Fonseca, J. M., Kitinoja, L. (2019): Postharvest Losses and Waste. p. 43. In: Yahia, E. M, Postharvest Technology of Perishable Horticultural Commodities. Woodhead Publishing. https://doi.org/10.1016/B978-0-12-813276-0.00002-X

[8] Morrow, C., Mohsenin, N. (1966): Consideration of Selected Agricultural Products as Viscoelastic Materials. Journal of Food Science 31 (5) pp. 686-698. https://doi.org/10.1111/j.1365-2621.1966.tb01925.x

[9] Tscheuschner, H., Doan, D. (1988): Modelling of mechanical properties of apple flesh under compressive load. Journal of Food Engineering 8 (3) pp. 173-186. https://doi.org/10.1016/0260-8774(88)90052-0

[10] Fenyvesi, L. (2004): Mezőgazdasági termények sérülésvizsgálata. Akadémiai Kiadó, Budapest.

[11] Szendrő, P. (2000): Mezőgazdasági Gépszerkezettan. Mezőgazdasági Szaktudás Kiadó, Budapest.

[12] Kim, J., Roque, R., Birgisson, B. (2006): Interpreting Dissipated Energy from Complex Modulus Data. Road Materials and Pavement Design 7 (2) pp. 223-245. https://doi.org/10.1080/14680629.2006.9690034

[13] Ghuzlan, K., Carpenter, S. (2000): Energy-Derived, Damage-Based Failure Criterion for Fatigue Testing. Transportation Research Record: Journal of the Transportation Research Board 1723 (1) pp. 141-149. https://doi.org/10.3141/1723-18

[14] Lee, J., Tan, J., Waluyo, S. (2016): Hysteresis characteristics and relationships with the viscoelastic parameters of apples. Engineering in Agriculture, Environment and Food 9 (1) pp. 36-42. https://doi.org/10.1016/j.eaef.2015.09.005

[15] Mohsenin, N. (1986): Physical properties of plant and animal materials. Gordon and Breach Science Publishers, Amsterdam.

[16] Sitkei, Gy. (1981): A mezőgazdasági anyagok mechanikája. Akadémiai Kiadó, Budapest.

[17] Li, Z., Miao, F., Andrews, J. (2017): Mechanical Models of Compression and Impact on Fresh Fruits. Comprehensive Reviews in Food Science and Food Safety 16 (6) pp. 1296-1312. https://doi.org/10.1111/1541-4337.12296

[18] Fischer, D., Craig, W. L., Watada, A. E., Douglas, W., Ashby, B. H. (1992): Simulated In-Transit Vibration Damage to Packaged Fresh Market Grapes and Strawberries. Applied Engineering in Agriculture 8 (3) pp. 363-366. https://doi.org/10.13031/2013.26078

[19] Hinsch, R. T., Slaughter, D. C., Craig, W. L., Thompson, J. F. (1993): Vibration of Fresh Fruits and Vegetables During Refrigerated Truck Transport. Transactions of the ASAE 36 (4) pp. 1039-1042. https://doi.org/10.13031/2013.28431

[20] Vursavuș, K., Özgüven, F. (2004): Determining the Effects of Vibration Parameters and Packaging Method on Mechanical Damage in Golden Delicious Apples. Turkish Journal Of Agriculture And Forestry 28 (5) pp. 311-320.

[21] Oveisi, Z., Minaei, S., Rafiee, S., Eyvani, A., Borghei, A. (2012): Application of vibration response technique for the firmness evaluation of pear fruit during storage. Journal of Food Science and Technology 51 (11) pp. 3261-3268. https://doi.org/10.1007/s13197-012-0811-z

[22] Vursavus K., Kesilmis Z., Oztekin B. (2017): Nondestructive dropped fruit impact test for assessing tomato firmness. Chemical Engineering Transactions 58, pp. 325-330.

[23] Petróczki, K., Fenyvesi, L. (2014): Improvement of compressive testing instrument with wide range of speed for examining agricultural materials. Computers and Electronics in Agriculture 101, pp. 42-47. https://doi.org/10.1016/j.compag.2013.12.003

[24] Pillinger, G., Géczy, A., Hudoba, Z., Kiss, P. (2018): Determination of soil density by cone index data. Journal of Terramechanics 77, pp. 69-74. https://doi.org/10.1016/j.jterra.2018.03.003

[25] Fenyvesi, L. (2004): Mezőgazdasági termények sérülésvizsgálata. Akadémiai Kiadó, Budapest.

[26] Delgadillo, R., Bahia, H. (2005): Rational fatigue limits for asphalt binders derived from pavement analysis. Asphalt paving thechnology: Journal of the association of asphalt paving technologics 74, pp. 1-42.

[27] Van Zeebroeck, M., Dintwa, E., Tijskens, E., Deli, V., Loodts, J., De Baerdemaeker, J., Ramon, H. (2004): Determining tangential contact force model parameters for viscoelastic materials (apples) using a rheometer. Postharvest Biology and Technology 33 (2) pp. 111-125. https://doi.org/10.1016/j.postharvbio.2004.02.008